

Efficient transportation of nano-sized particles along slotted photonic crystal waveguide

Pin-Tso Lin and Po-Tsung Lee*

Department of Photonics and Institute of Electro-Optical Engineering, National Chiao Tung University, Rm. 413
CPT Building, 1001 University Road, Hsinchu 300, Taiwan

*potsung@mail.nctu.edu.tw

Abstract: We design a slotted photonic crystal waveguide (S-PhCW) and numerically propose that it can efficiently transport polystyrene particle with diameter as small as 50 nm in a 100 nm slot. Excellent optical confinement and slow light effect provided by the photonic crystal structure greatly enhance the optical force exerted on the particle. The S-PhCW can thus transport the particle with optical propulsion force as strong as 5.3 pN/W, which is over 10 times stronger than that generated by the slotted strip waveguide (S-SW). In addition, the vertical optical attraction force induced in the S-PhCW is over 2 times stronger than that of the S-SW. Therefore, the S-PhCW transports particles not only efficiently but also stably. We anticipate this waveguide structure will be beneficial for the future lab-on-chip development

©2012 Optical Society of America

OCIS codes: (230.7380) Waveguides, channeled; (350.4238) Nanophotonics and photonic crystals; (350.4855) Optical tweezers or optical manipulation.

References and links

1. A. Ashkin, "Acceleration and trapping of particles by radiation pressure," *Phys. Rev. Lett.* **24**(4), 156–159 (1970).
2. A. Ashkin, J. M. Dziedzic, J. E. Bjorkholm, and S. Chu, "Observation of a single-beam gradient force optical trap for dielectric particles," *Opt. Lett.* **11**(5), 288–290 (1986).
3. S. Gaugiran, S. Gétin, J. M. Fedeli, G. Colas, A. Fuchs, F. Chatelain, and J. Dérourard, "Optical manipulation of microparticles and cells on silicon nitride waveguides," *Opt. Express* **13**(18), 6956–6963 (2005).
4. S. Kawata and T. Sugiura, "Movement of micrometer-sized particles in the evanescent field of a laser beam," *Opt. Lett.* **17**(11), 772–774 (1992).
5. M. Gu, J. B. Haumonte, Y. Micheau, J. W. M. Chon, and X. Gan, "Laser trapping and manipulation under focused evanescent wave illumination," *Appl. Phys. Lett.* **84**(21), 4236–4238 (2004).
6. V. Garcés-Chávez, K. Dholakia, and G. C. Spalding, "Extended-area optically induced organization of microparticles on a surface," *Appl. Phys. Lett.* **86**(3), 031106 (2005).
7. T. Čížmár, V. Garcés-Chávez, K. Dholakia, and P. Zemánek, "Optical conveyor belt for delivery of submicron objects," *Appl. Phys. Lett.* **86**(17), 174101 (2005).
8. M. J. Guffey, R. L. Miller, S. K. Gray, and N. F. Scherer, "Plasmon-driven selective deposition of au bipyramidal nanoparticles," *Nano Lett.* **11**(10), 4058–4066 (2011).
9. K. Okamoto and S. Kawata, "Radiation force exerted on subwavelength particles near a nanoaperture," *Phys. Rev. Lett.* **83**(22), 4534–4537 (1999).
10. L. Novotny, R. X. Bian, and X. S. Xie, "Theory of nanometric optical tweezers," *Phys. Rev. Lett.* **79**(4), 645–648 (1997).
11. A. Rahmani and P. C. Chaumet, "Optical trapping near a photonic crystal," *Opt. Express* **14**(13), 6353–6358 (2006).
12. M. Barth and O. Benson, "Manipulation of dielectric particles using photonic crystal cavities," *Appl. Phys. Lett.* **89**(25), 253114 (2006).
13. S. Kawata and T. Tani, "Optically driven Mie particles in an evanescent field along a channeled waveguide," *Opt. Lett.* **21**(21), 1768–1770 (1996).
14. B. S. Schmidt, A. H. J. Yang, D. Erickson, and M. Lipson, "Optofluidic trapping and transport on solid core waveguides within a microfluidic device," *Opt. Express* **15**(22), 14322–14334 (2007).
15. B. S. Ahluwalia, P. McCourt, T. Huser, and O. G. Hellesø, "Optical trapping and propulsion of red blood cells on waveguide surfaces," *Opt. Express* **18**(20), 21053–21061 (2010).
16. A. H. J. Yang, T. Lertsuchatawanich, and D. Erickson, "Forces and transport velocities for a particle in a slot waveguide," *Nano Lett.* **9**(3), 1182–1188 (2009).
17. A. H. J. Yang, S. D. Moore, B. S. Schmidt, M. Klug, M. Lipson, and D. Erickson, "Optical manipulation of nanoparticles and biomolecules in sub-wavelength slot waveguides," *Nature* **457**(7225), 71–75 (2009).

18. V. R. Almeida, Q. F. Xu, C. A. Barrios, and M. Lipson, "Guiding and confining light in void nanostructure," *Opt. Lett.* **29**(11), 1209–1211 (2004).
19. E. Yablonovitch, "Inhibited spontaneous emission in solid-state physics and electronics," *Phys. Rev. Lett.* **58**(20), 2059–2062 (1987).
20. T. F. Krauss, R. De La Rue, and S. Brand, "Two-dimensional photonic-bandgap structures operating at near-infrared wavelengths," *Nature* **383**(6602), 699–702 (1996).
21. T. F. Krauss, "Slow light in photonic crystal waveguides," *J. Phys. D: Appl. Phys.* **40**(9), 2666–2670 (2007).
22. A. Di Falco, L. O'Faolain, and T. F. Krauss, "Dispersion control and slow light in slotted photonic crystal waveguides," *Appl. Phys. Lett.* **92**(8), 083501 (2008).
23. A. Di Falco, L. O'Faolain, and T. F. Krauss, "Photonic crystal slotted slab waveguides," *Photon. Nanostructures* **6**(1), 38–41 (2008).
24. P. T. Lin and P. T. Lee, "All-optical controllable trapping and transport of subwavelength particles on a tapered photonic crystal waveguide," *Opt. Lett.* **36**(3), 424–426 (2011).
25. S. Y. Shi, C. H. Chen, and D. W. Prather, "Plane-wave expansion method for calculating band structure of photonic crystal slabs with perfectly matched layers," *J. Opt. Soc. Am. A* **21**(9), 1769–1775 (2004).
26. K. Grujic, O. G. Hellesø, J. P. Hole, and J. S. Wilkinson, "Sorting of polystyrene microspheres using a Y-branched optical waveguide," *Opt. Express* **13**(1), 1–7 (2005).
27. R. F. Marchington, M. Mazilu, S. Kuriakose, V. Garcés-Chávez, P. J. Reece, T. F. Krauss, M. Gu, and K. Dholakia, "Optical deflection and sorting of microparticles in a near-field optical geometry," *Opt. Express* **16**(6), 3712–3726 (2008).
28. S. Mandal, X. Serey, and D. Erickson, "Nanomanipulation using silicon photonic crystal resonators," *Nano Lett.* **10**(1), 99–104 (2010).
29. A. H. J. Yang and D. Erickson, "Stability analysis of optofluidic transport on solid-core waveguiding structures," *Nanotechnology* **19**(4), 045704 (2008).
30. J. D. Jackson, *Classical Electrodynamics* (Wiley, 1975), Chap. 6.

1. Introduction

Optical force has surpassed mechanical force in many biochemical applications. Especially in microscopic regime, the studied objects, such as proteins and viruses, are always tiny and easily damaged by mechanical contacts. Thus, optical force with contactless and nondestructive properties becomes the most suitable tool for handling tiny living things. After Ashkin's pioneering works in 1970s [1], gradient force optical trap, or called optical tweezers, realized trapping dielectric particles by optical force [2]. In which, highly-focused laser beam generates strong light-matter interaction and enhances optical force near the focus. However there are two limits making optical tweezers difficult to be integrated with sequential analyzing units and hindering lab-on-chip development. One is the short working distance of focusing system, which is an inevitable result of using objective lens with high numerical aperture to reduce the spot size. The other is the massive system volume compared to the space where objects are manipulated. Also, optical tweezers are not fit for parallel manipulation because it moves objects one by one [3]. Fortunately, researchers found that optical force induced by evanescent field can also manipulate objects at the interface of two media [4–8]. This overcomes the mentioned limits because evanescent field is not directly generated by focusing systems. Configurations utilizing optical force to manipulate particles in the near field thus started blooming. Nano-aperture, nano-tip, and optical cavities had shown their ability to trap particles, on chip, more precisely compared to focusing systems [9–12]. In 1996, Kawata *et al.* demonstrated that optical waveguides can also transport particles by the propagation nature of guided wave while attracting them into the evanescent field around the waveguides [13]. This structure is not only adapted for on-chip-integration and parallel manipulation, recently its ability to transport and sort objects simultaneously makes it attract much attention [14,15].

Gaugiran *et al.* had compared the induced optical forces on waveguides of different refractive indices under the same guided power [3]. For the same particle size, they found silicon nitride waveguide (refractive index $n = 1.97$) can transport particles with optical forces stronger than that generated by waveguides of lower refractive indices. Even so, particles merely interact with minor optical energy which extends into surrounding in evanescent form. For overcoming this drawback, Yang *et al.* introduced a slot structure into solid-core waveguides [16,17]. The slot creates a pseudo transverse-electric (TE) mode with major optical energy distributed within the accessible low-index region [18]. Thus particles can interact directly with strong guided power. However, there is still a structure, photonic crystal

(PhC), which can further enhance the interaction between optical field and particles. Many researches had shown that PhC can confine light within wavelength scale more efficiently by photonic band gap (PBG) effect than by total internal reflection (TIR) [19,20]. The periodicity along PhC waveguide also causes slope of the waveguide band approaching zero near the band edge, where slow light effect occurs and enhances light-matter interaction [21–23]. Based on these motivations, we had proposed that a tapered PhC waveguide can trap particles at a wavelength-dependent position [24]. Nevertheless, PhC waveguide so far has not been exploited in particle transportation. In this report, we incorporate a slot structure into PhC waveguide to transport particles. Together with the advantage of using slot structure, the excellent optical confinement and slow light effect will further improve the waveguide structure in particle transportation. We numerically show that our proposed design can serve as an efficient and stable transport system for the biological integration chip.

2. Waveguide design and simulation results

In our design, the slotted PhC waveguide (S-PhCW), as partially depicted in Fig. 1(a), is formed on a free-standing silicon slab (refractive index $n = 3.46$ and thickness $t = 250$ nm). We do not use the structure of silicon-on-insulator but use free-standing slab for reducing optical losses through the substrate in real situation. This structure is feasible for PhC waveguide because the dielectric connections between holes can sustain the waveguide and many works have realized the free-standing S-PhCW in fabrication [22, 23]. To simulate the real situation when manipulating biological objects, we assume the whole waveguide system is immersed in water surrounding ($n = 1.33$). The PhC structure is consisted of holes distributed in hexagonal lattice with lattice constant $a = 450$ nm and hole radius $r = 0.35a$. The waveguide is formed by eliminating a row of holes in Γ -K direction. A slot opened at center of the PhC waveguide core is 100 nm in width (w), which is sufficiently narrow for sustaining pseudo TE mode with field greatly enhanced in the slot. For single mode operation, we shift the holes, nearest to the slot, toward the waveguide center by $0.125a$. The remaining holes are shifted away from the waveguide center by $0.02a$ for band tailoring. We calculate the band diagrams by using three-dimensional (3D) plane-wave-expansion method [25]. Finally a smoothly curved waveguide band is tuned to the mid-gap of PBG as shown in Fig.

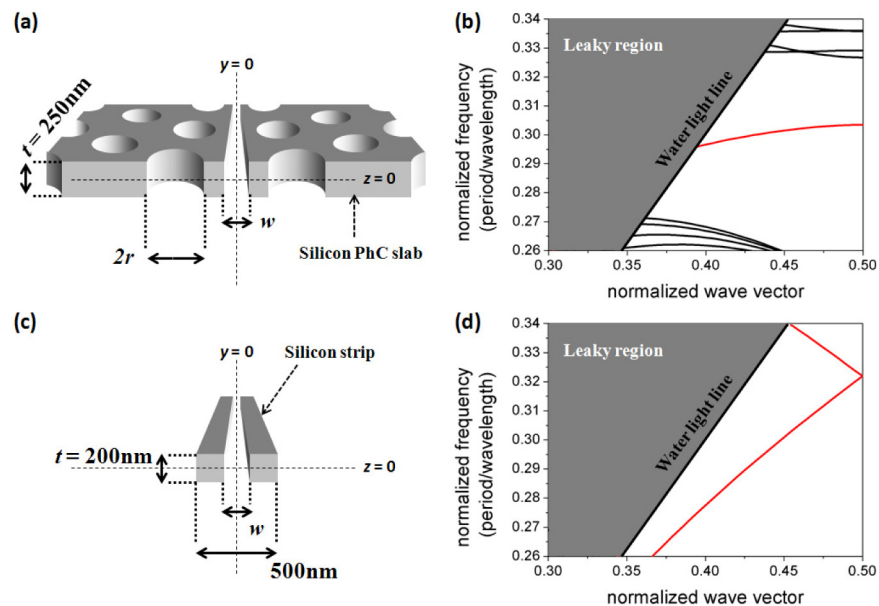


Fig. 1. (a) and (c) are schematic illustrations of the S-PhCW and the S-SW respectively. (b) and (d) are the corresponding band diagrams.

1(b). For $a = 450$ nm, edge of the waveguide band is at 1480 nm, where slope of the band approaches zero. The band slope represents group velocity of the guided wave. Thus slow light effect becomes prominent when the slope reduces. For wavelength shorter than 1480 nm, waves in the band gap region are forbidden to propagate along the waveguide. At the other end, the band tail enters the leaky region above water light line at 1520 nm. For wavelength longer than 1520 nm, waves would easily radiate into the water surrounding instead of being guided in the slab.

We also build a suspended silicon strip waveguide with a 100 nm slot opened at the center of the core as depicted in Fig. 1(c). Though this structure is impractical to be fabricated, we use it as the reference structure. Comparison between the S-PhCW and the slotted strip waveguide (S-SW) is thus on the same base that losses through substrate are reduced. The S-SW is designed as that in [16], where the waveguide is 500 nm in width and 200 nm in height. Figure 1(d) shows the band diagram of the S-SW with bands folded back into the first Brillouin zone. The frequency and wave vector are normalized as band diagram of the S-PhCW in Fig. 1(b). Because this structure has no periodicity along the direction of wave propagation, the bands do not anti-cross against each other as PhC waveguide bands. Thus for the S-SW, there is no band gap, and the waveguide bands are more oblique than PhC waveguide bands. Slow light effect will not occur in the S-SW.

For investigating abilities of the waveguides in particle manipulation (attract and transport), we use 50 nm polystyrene spheres ($n = 1.59$ around 1500 nm) as the target particle. Polystyrene has the properties of low absorption and low index contrast relative to water surrounding. Sub-micrometer sized polystyrene spheres are always used to mimic tiny biological objects, such as proteins and viruses [16, 26–28]. In this report, we simulate waves propagating along the waveguides and interacting with the particle by using 3D finite element method (Comsol Multiphysics software). We first use built-in boundary mode analysis in the software to calculate the guided modes, and then launch them into the waveguides. Optical force exerted on the particle can be calculated by integrating time averaged Maxwell stress tensor on the external surface of the particle [29, 30]. We set the coordinate system with $z = 0$ and $y = 0$ at vertical center of the slab and horizontal center of the slot respectively. Figure 2(a) shows the propulsive component of optical force (in the direction of wave propagation, x) when the particle is located at the slot center ($z = 0$ and $y = 0$) and 1 W power is coupled into the waveguides. For the S-SW, the propulsion force varies gently as a function of launching wavelength (blue curve in Fig. 2(a)). The strongest propulsion force is 0.44 pN/W at 1475 nm. However for the S-PhCW, the propulsion force varies drastically (red curve in Fig. 2(a)) in the wavelength range corresponding to the waveguide band. This feature is partially resulted from the excellent confinement provided by PhC structure. Quantitatively, we define a confinement factor as the percentage of power guided in the slot. In this wavelength range, the factor of the S-PhCW is at least 2.7 times higher than that of the S-SW as shown in Fig. 2(b). By comparing intensity profiles of the modes guided in the waveguides (Figs. 2(c) and (d)), it is easy to find that power guided along the S-PhCW is more concentrated in the slot. Thus the S-PhCW can exploit more optical power to interact with the particle. Furthermore, overall band slope of the S-PhCW is lower than that of the S-SW. The corresponding slow group velocity further enhances the interaction between guided waves and the particle. Therefore, the S-PhCW far surpasses the S-SW in propulsion force and will transport particle more efficiently in this wavelength range. At 1505 nm, the propulsion force reaches its peak value of 5.3 pN/W, which is over 10 times stronger than that in the S-SW. The extra enhancement (7.3 times, other than that caused by the better confinement) can be attributed to the slow light effect. Theoretically, slow light enhancement should be most prominent at the band edge.

However the peak propulsion force does not occur right at the band edge because coupling light into a mode with slower group velocity is more inefficient. For wavelength shorter than 1480 nm, no wave would interact with the particle. Thus the propulsion force drops rapidly and becomes negligible compared with that in the S-SW. For wavelength longer than 1520 nm, optical power radiates out of the slab more easily and wave interacts with the particle with less power. The propulsion force thus drops again.

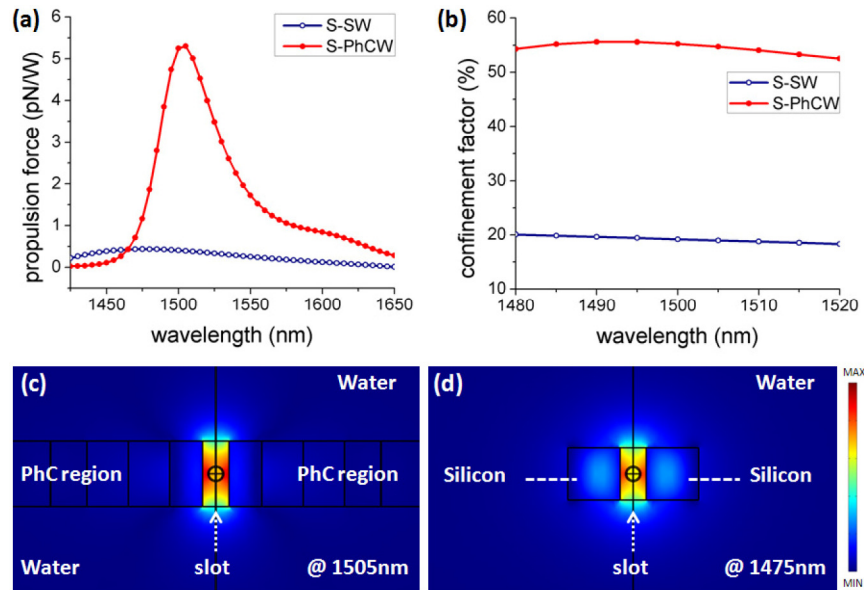


Fig. 2. (a) Propulsion forces exerting on the particle when it is located at slot center of the S-PhCW and S-SW. (b) Confinement factors of the waveguides. (c) and (d) are intensity profiles of waves guided along the S-PhCW and S-SW respectively.

For verifying that particles can be stably transported along the slot, we proceed to simulate the optical force with the particle at different vertical positions z in the slot ($y = 0$). Wavelengths excited in the S-PhCW and the S-SW are at 1505 nm and 1475 nm respectively, where the propulsion force is the strongest for each waveguide. Figure 3(a) shows the vertical component of optical force (in z direction) as a function of z . The vertical force is negative for $z > 0$, which means particles located above the slab center (plane of $z = 0$) would be attracted downward. Because the waveguide structures are symmetric vertically, optical force exerted on the particle is mirror symmetric with respect to the slab center. Therefore, the vertical force will be positive and will attract the particle upward when $z < 0$. Finally the particle in the slot will be attracted at the slab center, which is the equilibrium position with upward and downward forces canceled out to zero. Due to this attraction property, the restoring vertical force is also called optical attraction force. When some perturbation floats the particle slightly away from the slab center, strength of the attraction force increases progressively to pull the particle back and attains a peak value. For the S-PhCW and the S-SW, the peaks are at $z = 125$ nm and 100 nm respectively. These positions are upper entrance of the slots (half of the waveguide thickness) where the particle will experience a sharp transition of optical energy as shown in the insets. Due to the excellent confinement and the slow light enhancement provided by PhC structure, the S-PhCW surpasses the S-SW in attracting particles vertically. The attraction force induced in the S-PhCW is over 2 times stronger than that in the S-SW. When the particle floats away further, the guided wave will lose its effect upon the particle. The strength of attraction force declines along z , which represents the characteristic of evanescent field. These features are the same for the particle positioned below the slab center.

By integrating the attraction force along z axis (from $z \gg 0$ toward $z = 0$), we can get the corresponding potential U when 1 W power is coupled into the waveguides. Here the zero potential is defined as when the particle is away from the slab center for 2 μm , where the evanescent optical energy had already died out. We plot the potential distribution from $z = 0$ to $z = 300$ nm in Fig. 3(b). In the slab region, the potential distributes as a well, which is even-symmetry with respect to $z = 0$. A criterion widely used for stable trapping is that depth ΔU of the potential well must be larger than $10k_B T$ [2], where k_B is the Boltzmann constant and T is

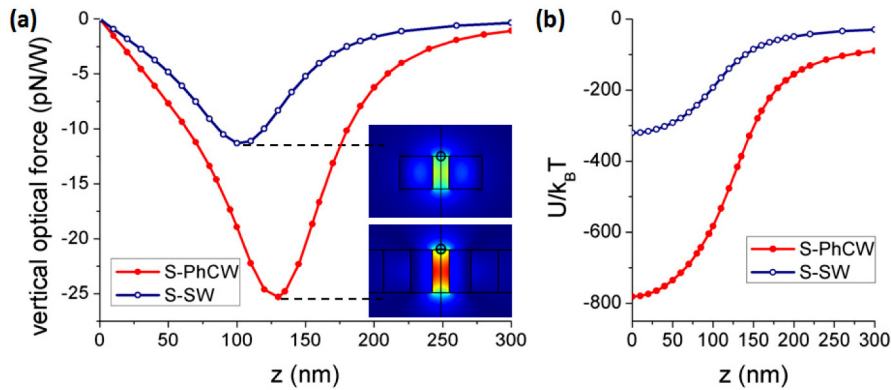


Fig. 3. (a) Vertical optical force exerting on the particle at different vertical positions z in the slot. Wavelengths excited in the S-PhCW and the S-SW are at 1505 nm and 1475 nm respectively. Insets are the corresponding intensity profiles when the particle is at the slot entrance. (b) Potentials experienced by the particle in the S-PhCW and S-SW.

the system temperature. Here we set T to be room temperature 300k. When the criterion is satisfied, the attraction force would overcome the Brownian motion caused by random thermal perturbation. And the waveguide will transport particles stably without being easily disturbed. For S-PhCW, the lowest power required for stable trapping ($\Delta U = 10k_B T$) is only 12.8 mW, which will generate 0.068 pN propulsion force. However it is 31.2 mW for the S-SW, and merely 0.014 pN propulsion force is generated. Therefore the S-PhCW can stably attract particles in the slot at a lower power and can transport particles with stronger propulsion force.

We also simulate the situation when the particle is above the surface of the waveguides by 5 nm and at different horizontal positions y . The S-PhCW and S-SW are operated at 1505 nm and 1475 nm respectively. Figure 4(a) shows the horizontal component of optical force (in y direction) as a function of y . The horizontal component is also a restoring force as the vertical attraction force. Therefore when the particle is positioned at positive y , the horizontal force component will be negative and will attract the particle toward the slot center ($y = 0$). The force becomes the strongest near edge of the slot ($y = 50$ nm) where the particle experiences sharp transition of optical energy. Again, owing to the excellent optical confinement and the slow light enhancement provided by PhC structure, the S-PhCW surpasses the S-SW in attracting particles horizontally. The corresponding potential distributions shown in Fig. 4(b)

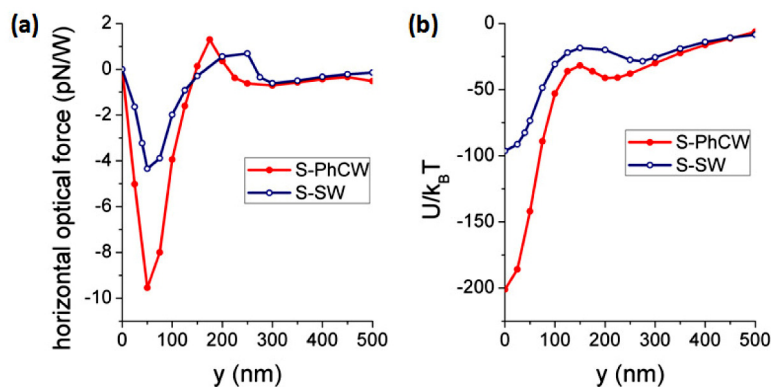


Fig. 4. (a) Horizontal optical force exerting on the particle at different horizontal positions y when it is above the waveguide surface by 5 nm. The S-PhCW and S-SW are operated at 1505 nm and 1475 nm respectively. (b) Potentials experienced by the particle in the S-PhCW and S-SW.

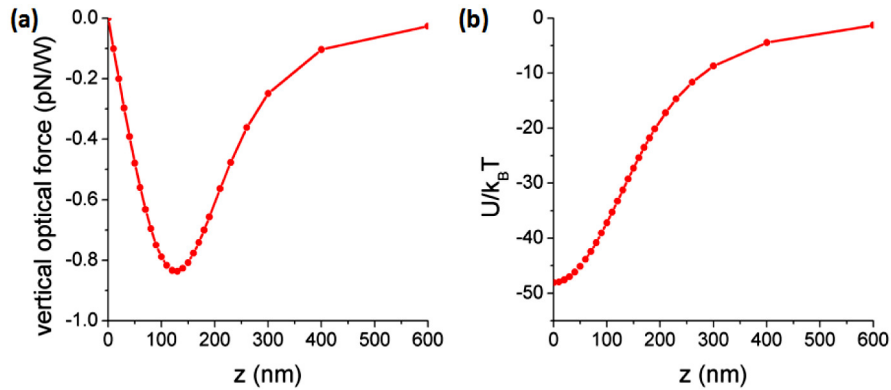


Fig. 5. (a) Vertical optical force exerting on the particle in the hole nearest to the slot of the S-PhCW at different vertical positions z . The excited wavelength is 1505 nm. (b) Potential experienced by the particle.

also indicate that the S-PhCW can attract particles in the slot region more stably than the S-SW can do.

To verify that the particles will not be trapped in the holes of PhC structure but will be transported along the slot, we simulate the optical force with the particle in a hole nearest to the slot. The excitation wavelength is 1505 nm, and the power coupled into the waveguide is 1 W. Figure 5(a) shows the vertical force exerted on the particle when it is at different vertical positions z on the central axis of the hole. The features are the same as those obtained when the particle is in the slot. The vertical force will attract the particle toward the slab center (plane of $z = 0$), where the vertical forces are canceled out. When the particle floats away from the slab center, the attraction force (restoring vertical force) first becomes stronger and attains its peak at entrance of the hole ($z = 125$ nm). Then it declines along z representing the characteristic of evanescent field. However, the peak strength of attraction force is merely 0.84 pN, which is far smaller than that exerting on the particle when it is in the slot. Figure 5(b) shows the corresponding potential experienced by the particle. When the power coupled into the waveguide is 12.8 mW ($\Delta U = 10k_B T$ for stably trapping the particle in the slot), potential depth in the hole is merely $0.62k_B T$. This means particles attracted into the holes will easily float out through Brownian motion. Therefore holes of the PhC structure will not hinder the particles from being transported along the S-PhCW. The efficient and stable transport ability of the proposed S-PhCW design will make it very suitable for transporting particles between functional analyzing units in the future biological integration chip.

3. Summary

We propose an S-PhCW design for transporting particles by the guided optical wave. 3D finite element method is used to simulate the interaction between guided wave and particle. Comparing to TIR confinement, PhC structure can further concentrate the guided power into the slot. Confinement factor of the S-PhCW, over its band wavelength range, is at least 2.7 times higher than that of the S-SW. Thus more power can be utilized to interact with particles in the slot. Moreover, the periodicity of PhC structure makes slow light effect occur in the S-PhCW. This further enhances the interaction between guided wave and particles. For transporting polystyrene particles as small as 50 nm, the S-PhCW generates propulsion force as strong as 5.3 pN/W, which is over 10 times stronger than that generated by the S-SW. In addition, the vertical attraction force induced in slot of the S-PhCW is over 2 times stronger than that of the S-SW. Therefore particles can be transported more efficiently and stably along the S-PhCW, which will be beneficial for the development of future lab-on-chip system.

Acknowledgments

This work is supported by Taiwan's National Science Council (NSC) under contract numbers NSC-100-2221-E-009-109-MY3 and NSC-100-2120-M-009-005.